Carcinogenesis vol.32 no.9 pp.1324–1332, 2011
doi:10.1093/carcin/bgr127
Advance Access publication July 5, 2011

Pleural mesothelioma side populations have a precursor phenotype

Claudia Frei, Isabelle Opitz[1], Alex Soltermann[2], Bruno Fischer, Ubiratan Moura, Hubert Rehrauer[3], Walter Weder[1], Rolf Stahel and Emanuela Felley-Bosco*

Laboratory of Molecular Oncology, Clinic of Oncology, University Hospital Zürich, Haeldeliweg 4, 8044 Zurich, Switzerland, [1]Division of Thoracic Surgery, and [2]Institute of Surgical Pathology, University Hospital Zürich, Haeldeliweg 8091 Zürich, Switzerland and [3]Functional Genomic Center Zurich, 8057 Zurich, Switzerland

*To whom correspondence should be addressed. Tel: +41 44 6342878; Fax: +41 44 6342872;
Email: emanuela.felley-bosco@usz.ch

DyeCycleViolet was used to set up the side population (SP) functional assay aimed at identifying subpopulations of malignant pleural mesothelioma (MPM) tumor cells with chemoresistance phenotype associated with ABCG2 transporter activity. Self-renewal, chemoresistance and tumorigenicity were tested for SP and non-side population (NSP) cells. Tumors were characterized by mesothelin, calretinin, N-cadherin, D2-40 and Wilms tumor 1 (WT1) immunohistochemistry. Surface expression of mesenchymal stem cell markers CD90, CD73 and CD105 was investigated in SP and NSP cells. We identified SP cells with self-renewal properties and increased chemoresistance in MPM cell lines and tumor-derived primary cell cultures. Compared with the non-SP fraction (NSP), the SP fraction led to the development of tumors including cells with mesothelium precursor phenotype characterized by mesenchymal morphology, being WT1 negative but cytoplasmic D2-40 positive and having a tendency of increased tumorigenicity. The same phenotypic shift was observed in patients with relapsing tumors after chemotherapy. Furthermore, the SP cells were enriched in $CD105^{-/low}$ expressing cells, which were small sized and had increased tumorigenicity compared with $CD105^{high}$ cells. Taken together, our results support the hypothesis that MPM $CD105^{-/low}$, chemoresistant small sized SP cells may constitute the cellular pool out of which recurrence develops. Further characterization of mechanisms of chemoresistance and self-renewal should lead to targets specific for this subpopulation in MPM patients.

Introduction

Asbestos-related malignant pleural mesothelioma (MPM) is expected to peak in 2020 (1). Survival rates are still ∼1 year (depending on the age and treatment) after diagnosis (2). Objective chemotherapy response is achieved in <50% of patients and has limited duration (3).

In order to gather a better understanding of MPM biology, which may ultimately help defining better therapeutic strategies, we considered parallel aspects between MPM development and other tumors linked to chronic injury (4). The asbestos fibers-induced MPM development is due to accumulation of inhaled asbestos fibers in the pleural space and subsequent damage of the mesothelium (5). Chronic tissue repair follows activating stem cell signaling pathways to regenerate the tissue but, because of persistent system stimulation, oncogenic events occur leading to tumor formation (reviewed in ref. 6). The presence within the latter of a population of cancer stem cells (CSC) highly resistant to chemotherapy might be the cause of tumor recurrence. Hence, the aim of our study was originally to identify and characterize MPM CSC. The latter, which have the capability to create exact tumor phenocopies when transplanted from one mice to the next, have been proposed to exist (7) based on the pioneer work identifying leukemic stem cells as $CD34^{+}/CD38^{-}$ cells, like hematopoietic stem cells (HSCs) in human acute myeloid leukemia (8,9). The presence of CSCs in solid tumors was identified for the first time as a small subset of heterogeneous breast cancer cells which were phenotypically distinct and characterized as $CD44^{+}/CD24^{-/low}$ (10). Since then, for many solid tumors, CSCs have been identified using corresponding tissue stem cell surface markers (reviewed in ref. 11). Normal mesothelium stem cell surface markers are not yet available to identify potential MPM CSCs. Hence, we used a functional assay, which identifies a small and distinct subset of cells called 'side population' (SP), with phenotypic markers of multipotential HSC after staining bone marrow with the DNA staining dye Hoechst 33342 (12). The SP is due to the expression of functional adenosine triphosphate-binding cassette (ABC) transporters (13). When living cells are stained with Hoechst 33342, SP cells do efflux the DNA-staining dye via their ABC transporters. When cells are coincubated with ABC transporter inhibitors verapamil or fumitremorgin C, Hoechst 33342 is no longer effluxed leading to a shift in the dual emission wavelength fluorescence-activated cell sorting (FACS) analysis upon which the SP can be identified. The ABCG2 drug transporter is responsible for the SP in the bone marrow (13,14). Although this assay has already been applied to mesothelioma cell lines (15), several issues are still needed to be addressed. Firstly, self-renewal of sorted SP has not been investigated yet, second tumorigenicity has been determined only for SP and NSP cells sorted from MS-1 cell line, which has a biphasic histotype and no differences were found. In our study, those questions were addressed using primary cultures from xenografts, either from a cell line or from a patient-derived tumor instead of cell lines. In addition, surface phenotype and chemoresistance were characterized.

Abbreviations: ABC, adenosine triphosphate-binding cassette; CSC, cancer stem cell; DCV, DyeCycleViolet; EDTA, ethylenediaminetetraacetic acid; FACS, fluorescence-activated cell sorting; FCS, fetal calf serum; HSC, hematopoietic stem cell; MPM, malignant pleural mesothelioma; SP, side population; NSP, non-side population; PBS, phosphate-buffered saline.

Material and methods

Tissue samples

Human tumor specimens were obtained and processed as described previously (16,17).

Cell lines and primary cell cultures

The human promyelocytic leukemia cell line HL60/Dox selected by chronic exposure to doxorubicin was kindly provided by Dr M.Andreev (Department of Blood and Marrow Transplantation, UT MD Anderson Cancer Center, Huston, TX) and maintained in RPMI 1640 (Sigma–Aldrich, Buchs SG, Switzerland) supplemented with 10% fetal calf serum (FCS) (Omnilab, Mettmenstetten, Switzerland), 1% penicillin/streptomycin and 1 mM L-Glutamine (both obtained from GIBCO, Basel, Switzerland). The breast cancer cell line MCF-7 was maintained in RPMI 1640 supplemented with 10% FCS, 1% penicillin/streptomycin and 2 mM L-Glutamine. Primary MPM cell cultures were established from surgical specimens or xenografts as follows: tumors were blended into small pieces of 1–3 mm^2, then fragments were directly added to culture medium adapted from Connell *et al.* (18) (Dulbecco's modified Eagle's medium/F12 + GlutaMax (GIBCO), 15% FCS, 0.4 μg/ml hydrocortisone (Sigma–Aldrich), 10 ng/ml epidermal growth factor (GIBCO), 1% ITS (insuline, transferrin, selenium; GIBCO), 1 mM sodium pyruvate (Sigma–Aldrich), 100 μM beta-mercaptoethanol (Fluka, Buchs SG, Switzerland), supplemented with 1% non-essential amino acids (GIBCO) and 30% conditioned medium) or were incubated with collagenase 3 (200 U/ml; Worthington Biochemical Corporation, Lakewood, NJ) and hyaluronidase (100 U/ml) for 6 h at 37° C followed by digestion with 0.25% Trypsin/ethylenediaminetetraacetic acid (EDTA; GIBCO) for 2 min at 37°C and with 20 mg/ml DNAseI (Worthington Biochemical Corporation) for additional 2 min at 37°C. At the end of the collagenase digestion, tissues were filtered through a 70 μm cell sieve. The filtrate was centrifuged and the pellet resuspended in culture medium. The mesothelioma cell lines ZL34 and ZL55 were established in our laboratory (19). The MPM cell line H28 and Met5A, a mesothelial cell line obtained by SV40 transformation of mesothelial cells (20), were obtained

from ATCC. All cell lines used in this study were authenticated by DNA fingerprinting (Microsynth, Balgach, Switzerland).

Gene expression analysis

Selected gene expression analysis was performed as described previously (16,17). Additional primers are listed in the Supplementary Table I, available at *Carcinogenesis* Online. The heatmap was produced with *R* using default options on ΔC_t raw data. We used the logarithmic expression values and subtracted for each gene its mean expression.

Measurement of cell growth

To test sensitivity to mitoxantrone, cells were first incubated for 1 h with mitoxantrone (Sigma–Aldrich) (1 ng/ml) then verapamil (20 μM) was added or not for 1 h. Both drugs were suspended in medium without serum. After incubation, drugs were removed and cells were grown for further 3 days in serum containing medium. Sensitivity to cisplatin (0–16 μM) was tested in MPM medium containing 0.5% FCS. Cell growth was determined as described previously (21).

Western blot analysis

Western blotting was done as described (16). The western blots are representatives of two to five independent experiments.

SP analysis

Cells were stained with DyeCycleViolet (DCV) using a method described previously (22–24) and adapted as follows. Briefly, cells were washed with phosphate-buffered saline (PBS), trypsinized and resuspended in Dulbecco's modified Eagle's medium:F12 supplemented with 2% FCS, 10 mM 4-(2-hydroxyethyl)-1-piperazineethanesulfonic acid (HEPES; Sigma–Aldrich), 0.4 μg/ml hydrocortisone, 10 ng/ml epidermal growth factor, 1% ITS, 100 μM β-mercaptoethanol, 1 mM sodium pyruvate, 2 mM L-Glutamin and 1% non-essential amino acids. As positive controls, HL60/Dox cells were used. Cells were incubated with DCV (0.5 μM; Invitrogen, Basel, Switzerland) in the absence or presence of verapamil (50 μM; Sigma–Aldrich) at 37°C for 90 min in the dark mixing every 15 min. Then, cells were spin down at 4°C and resuspended in ice-cold Hanks' balanced salt solution (HBSS; GIBCO) supplemented with 10 mM HEPES and 5 mM EDTA (Amresco). Viable cells were gated with propidium iodide (PI; 2 μg/ml). Cells were gated on the FACSAria (Becton Dickinson, Allschwil, Switzerland) Forward Scatter Channel and Side Scatter Channel, a live gate was placed on cells excluding propidium iodide (Excitation 488 nm, Emission 610/20 nm) and single cells were gated based on Forward Scatter Channel (Forward Scatter Channel line versus pulse width) and Side Scatter Channel (Side Scatter Channel line versus pulse width). SP was determined by a gate placed on 450/40 versus 530/30 nm emission dot plot on a logarithmic amplified fluorescence scale after DCV excitation at 407 nm (25). The SP gate was identified using verapamil which blocks drug efflux. These settings gave the same results as 450/40 versus 650 nm longpass and allowed a direct comparison with results on surface phenotyping using the CyAn ADP analyzer (Beckman Coulter, Nyon, Switzerland), described below where only the 530/40 nm filter for 405 nm excitation was available. After sorting, cells were cultured or processed for mice xenografts.

Immunohistochemistry

De-paraffinized sections were subjected to antigen retrieval using Tris/EDTA (1 mM/0.1 mM, pH9) or pepsin digestion (for WT1). Following quenching in 0.3% H_2O_2 (20 min) and permeabilization in 0.05% Saponin (5 min; Fluka), blocking was performed in 2% bovine serum albumin in PBS with 1% horse serum (20 min; Vector Laboratories) at room temperature. Sections were incubated with primary antibodies (in supplementary figures: N-cadherin 6G11, 1:50; DAKOCytomation, Baar, Switzerland; mesothelin 5B2, 1:30; NovoCastra™ Laboratories and calretinin 1:50, Abcam, Cambridge, UK) overnight at 4°C. Negative controls were incubated with secondary biotinylated antibody only (Vectastain® Elite® ABC Kit; Vector Laboratories, Servion, Switzerland). Sections were washed with PBS and incubated with secondary biotinylated antibody for 45 min at room temperature. Staining was visualized using 3,3′-diaminobenzidine tetrahydrochloride (Sigma–Aldrich), counterstained with Vector® Hematoxilyn QS (Vector Laboratories) and analyzed either using a Leica DM IRBE microscope and image acquisition with Nikon Coolpix and Retiga Cooled Color 12-bit camera and QCapture (QImaging) or using a Zeiss Mirax Midi Slide Scanner and image acquisition with a 3 CCD color camera and Mirax Viewer (Zeiss, Feldbach, Switzerland). A minimum of 200 cells was evaluated.

Surface phenotyping

Cells resuspended in ice-cold PBS/2 mM EDTA were incubated with antibodies against CD105 (SN6, allophycocyanin labeled; eBioscience, Vienna, Austria), CD90 and CD73 (5E10 and AD2, respectively, both phycoerythrin labeled; BD Bioscience, Allschwil, Switzerland) and podoplanin (purified, kindly provided by Dr D.Kerjaschki, Clinical Institute for Pathology, Medical University of Vienna, Vienna, Austria) and with allophycocyanin labeled, phycoerythrin labeled and purified IgG controls (eBioscience and BD Bioscience, respectively) at 4°C for 30 min in the dark. Secondary antibody (phycoerythrin labeled; Dianova, Rheinfelden, Switzerland) for podoplanin analysis was incubated at 4°C for 30 min in the dark. After washing with PBS cells were resuspended in ice-cold PBS/2 mM EDTA and analyzed. $CD105^{-/low}$ and $CD105^{high}$ cells were identified and electronically gated on either the FACSAria cell sorter or the CyAn ADP analyzer (Beckman Coulter) after allophycocyanin excitation at 633 nm. The purity of sorted cells was verified directly after sorting and was >98%.

Where additionally SP was investigated, cells were treated for the SP analysis prior to antibody incubation.

The expression of ABCG2 on the cell surface was verified by FACS analysis as described (26).

MPM xenografts into NOD/SCID mice

NOD/SCID mice were bred and maintained under conditions approved by the Animal Care Committee. Sorted cells were resuspended in Matrigel (Matrigel Basement Membrane Matrix; Becton Dickinson) and injected under the renal capsula of 6–8 weeks old mice that were irradiated with one Gray 1 day before injection (27). Tumor tissues obtained from patients were directly implanted under the renal capsula. The mice were anesthetized with isoflurane while cells were injected. All animals were killed between 13 and 21 weeks posttransplantation. Tumor volume in cubic centimeters was determined using the formula (length × width^2)/2, where length was the longest axis and width being the measurement at right angles to the length.

Results

Identification and characterization of a SP in the MMPM cell line ZL55

In preliminary experiments, we established an SP protocol using as an experimental control (28) the leukemia cell line HL60/Dox, which over expresses multidrug resistance proteins, allowing the cells to efflux the DNA staining dyes Hoechst 33342 or DCV. We observed that using DCV, which has the advantage of being excited at non-UV wavelength with an enhanced emission signal compared with Hoechst 33342 (23) resulted in a better separation of SP/NSP (Supplementary Figure 1A is available at *Carcinogenesis* Online). In addition, we found that DCV could be used at a concentration (0.5 μM) not toxic to cells (supplementary Figure 2 is available at *Carcinogenesis* Online), allowing to take into account the cytotoxicity concerns about this method (29). This DCV protocol was first applied to breast cancer cell line MCF-7 (30) to provide an additional control for low abundance SP (supplementary Figure 1B available at Carcinogenesis online and Table I).

Using the DCV protocol for the MPM cell line ZL55 (gating strategy presented in supplementary Figure 3, available at *Carcinogenesis* Online), we identified an SP of 2.1 ± 1.9% (n = 31, mean ± SD, Figure 1A and Table I), which was decreased by the drug transporter inhibitor verapamil, indicating that these cells represented the SP cells. To examine whether SP cells could regenerate SP and NSP cells, ZL55 cells were sorted into SP and NSP and further cultured *in vitro*. Reanalysis of ZL55 SP and NSP in respect to their SP/NSP distribution revealed that ZL55 SP was able to regenerate an SP (2.25%, n = 2), whereas only NSP (n = 2) was obtained with ZL55 NSP. These data suggest that an SP with self-renewal properties is present in MPM ZL55 cells. In addition, the ZL55 SP was enriched with cells expressing the drug transporter ABCG2 at both protein and messenger RNA level (Figure 1B). To further characterize SP versus NSP derived populations, the expression of N-cadherin and mesothelin, which we routinely use to characterize our primary cultures (16), were investigated. Both N-cadherin and mesothelin (Figure 1C, left panel) were not detected in ZL55 SP cells in which a higher relative expression of Sox2 was observed (Figure 1D). This might indicate that ZL55 SP cells are in a less differentiated state. The relative expression of MDR1 was also increased in the SP fraction (Figure 1D), which is not surprising given the fact that DCV is a substrate of various ABC transporters. Relative expression enrichment was also observed for ABCC3 but not for ABCC1. All in all, these data indicate that an SP with stem/progenitor cell properties is present in ZL55 cells.

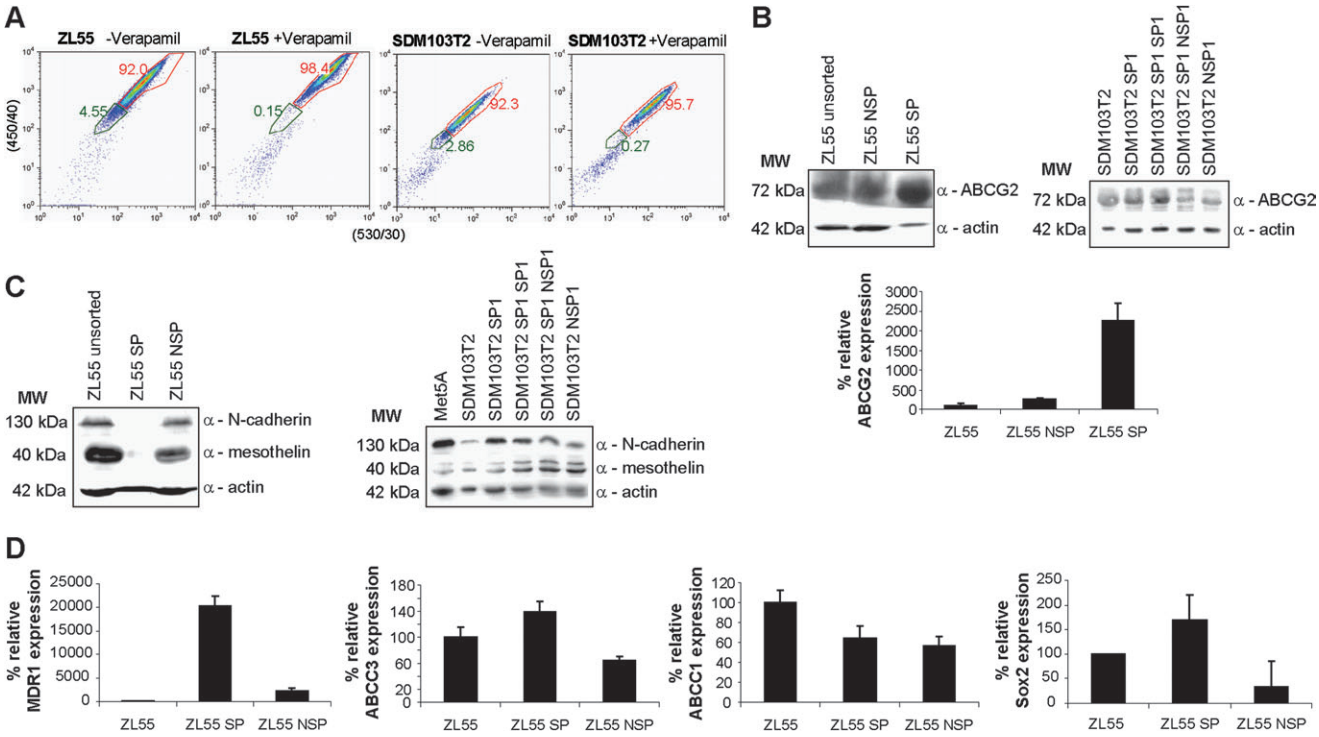

Fig. 1. ABCG2 and mesothelioma markers expression in the SP of an MPM cell line and a primary MPM xenograft cell culture **(A)** MPM cell line ZL55 and xenograft SDM103T2 cells were stained with DCV (0.5 μM) in the absence (−) or presence (+) of verapamil (50 μM). The SP (green gate) was defined as the population decreasing by the addition of verapamil. **(B)** Western blot and real-time polymerase chain reaction (PCR) analysis to assess ABCG2 expression levels in sorted SP and NSP cells. ABCG2 protein (BXP-21, 1:1000, Alexis Biochemicals, Lausen, Switzerland) was elevated in both ZL55 and SDM103T2 SP cells compared with NSP and parental cells. ABCG2 messenger RNA was also enriched in ZL55 SP cells. **(C)** Western blot analysis to determine the expression of mesothelin (MN-1, 1:1000; Rockland, Gilbertsville, PA) and N-cadherin (32/N, 1:2500; BD Bioscience) mesothelioma markers. Met5A cells were used as positive control for these two mesothelioma differentiation markers. Mesothelin was decreased in exponentially growing sorted SP cells. N-cadherin was also decreased but only in ZL55 SP cells. **(D)** Real-time PCR analysis revealed higher MDR1, ABCC3 and Sox2 messenger RNA expression in ZL55 SP compared with NSP cells. Real-time PCR data were normalized to histones and expressed as mean ± SD ($n = 3$). Actin (C4, 1:10 000; ICN) was used as western blot loading control.

Table I. Average SP abundance

Cell line		Average SP (%)	Number of replicates
Breast cancer[a]	MCF-7	2.3 ± 0.5	5
MPM	ZL55	2.1 ± 1.9	31
	ZL34	0.4 ± 0.1	3
	H28	0.7 ± 0.3	4
Primary MPM	SDM96	1.1	2
	SDM100	1.1	2
	SDM103T2	1.6 ± 1.5	24
	SDM138	0.2 ± 0.2	3
Primary mesothelial cells	SDM104	2.8	2

[a]Used as control (28).

Characterization of SP in additional MPM cell lines, MPM primary cell cultures and in a primary mesothelial cell culture

Beside the mesothelioma cell line ZL55, we investigated the SP distribution in two additional MPM cell lines ZL34 and H28, in three primary MPM cell cultures SDM96, SDM100 and SDM138, in a xenograft derived primary MPM cell culture SDM103T2 (Figure 1A) and in a primary mesothelial cell culture SDM104. In all these cell lines and primary cell cultures, an SP was identified (Table I).

The fact that an SP is also present in the primary mesothelial cell culture SDM104 indicates that a fraction of cells with potential self-renewal capacity is present in cultured normal mesothelium.

SDM103T2 cells were selected for further characterization for two reasons: firstly, they were derived from xenograft implantation of a tumor after chemotherapy, offering the opportunity to detect chemotherapy resistant cells. Secondly, tissue of relapsed tumor from the same patient was also available for further comparison. As for ZL55 cells, the SDM103T2 SP (Figure 1B, right panel) showed increased expression of ABCG2 and was able to regenerate a next SP (2.25%, $n = 1$) when cultured. The latter (SDM103T2 SP1 SP1, Figure 1B) was even further enriched for ABCG2 expression compared with the remaining NSP (SDM103T2 SP1 NSP1). Similarly to ZL55 cells, the expression of the MPM marker mesothelin was lower in SP compared with NSP (Figure 1C, right panel) while this trend was not observed for N-cadherin. Thus, it seems that SP phenotype is accompanied by decreased expression of mesothelin, which is generally abundantly expressed in epithelioid MPM (31). No specific enrichment of other ABC transporters in the SP fraction was observed (data not shown).

SP cells tend to be more tumorigenic than NSP cells

To test whether the tumorigenicity of SP and NSP differs, various numbers (10^2–10^5) of sorted ZL55 cells were injected under the renal capsule of NOD/SCID mice and monitored for tumor development. Both ZL55 SP and NSP gave rise to tumors when 10^5 cells were implanted ($n = 4$). By decreasing the injected cell number $<10^3$, neither ZL55 SP nor NSP gave rise to tumors ($n = 2$). Injecting between 10^3 and 10^4 cells of ZL55, SP and NSP led to tumor development for both SP and NSP in three of four mice tested. Therefore, similar to another study (15), no difference in a cell line SP versus NSP tumorigenicity was observed. We then injected sorted SP and NSP cells derived from an SP (ZL55 SPT) and an NSP (ZL55 NSPT3-3) tumor. Both cell cultures gave rise to an SP fraction (0.9 ± 0.7% and 0.2 ± 0.1%, $n = 8$ and $n = 3$, respectively). By injecting between 10^3 and 10^4 of these tumors′-derived sorted cells, there was a tendency (Figure 2A) to observe tumor formation more frequently with the SP

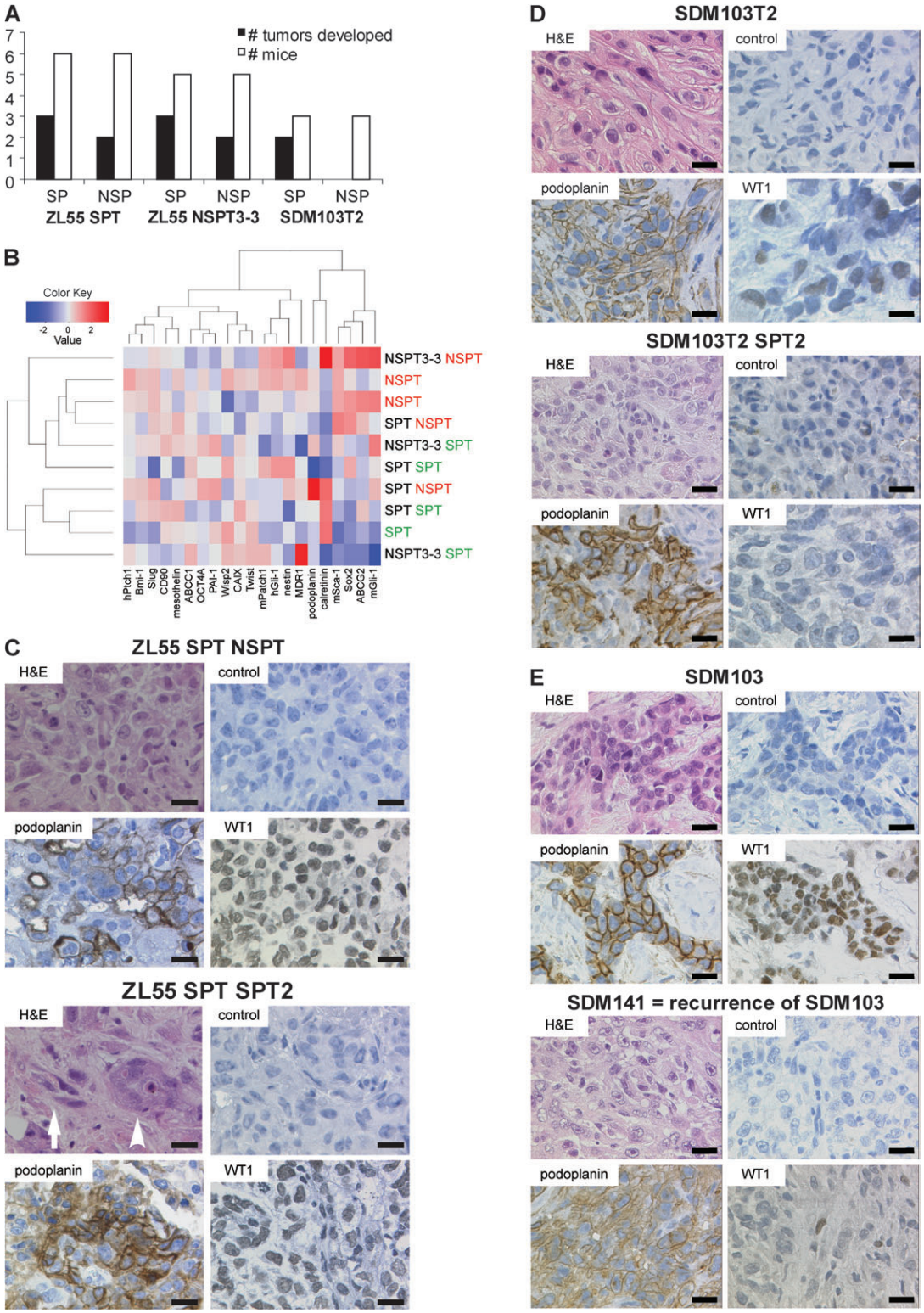

Fig. 2. Different phenotypes in freshly sorted SP/NSP and their derived tumors (**A**) SP from xenograft-derived tumors were enriched for tumor forming capacity in NOD/SCID mice. About 10^3–10^4 cells were implanted under the renal capsula of 1 Gy-irradiated mice. (**B**) Unsupervised clustering of SP- and NSP-derived tumors. Analyzed genes include ABC transporters ABCG2, MDR1 and ABCC1; stem cell markers Sox2, nestin, OCT4A, Bmi-1 and CD90; sonic hedgehog activity markers Gli-1, Patch1; hypoxia-controlled CAIX and Wisp2 and matrix-remodeling Slug, Twist and PAI-1. Matrix of relative gene expression values is shown as heatmap. Red indicates downregulated genes, blue indicates upregulated genes. (**C** and **D**) Representative tumors stained with either hematoxylin and eosin (H&E), without primary antibody (control) or with antibodies against WT1 (6F-H2, 1:50; DAKOCytomation) or podoplanin (D2-40, 1:50; DAKOCytomation). WT1 expression decreased in SP-derived tumor tissues, whereas podoplanin shifted from the membrane to the cytosol compared with NSP-derived tumor tissues for ZL55 cells and SDM103T2 tumor. In ZL55 SPT SPT2 (H&E), arrow denotes spindeloid tumor moiety, whereas arrowhead represents epitheloid mesothelioma (**E**) Tumor relapsing in patient SDM103 shifts toward mesothelium precursor phenotype defined as the absence of WT1 expression, increased podoplanin cytosolic staining and spindeloid phenotype. The scale bar represents 20 μm except for WT1 in SDM103T2 and SDM103T2 SPT2 (12.5 μm).

fraction. For the xenografted tumor-derived SDM103T2 only, SP cells gave rise to tumors. All in all, there is a tendency ($P = 0.12$, two-tailed chi-square test) for the SP fraction to have higher tumor initiating ability (8/14) compared with NSP fraction (4/14).

The existence of intrinsic differences between SP- and NSP-sorted cells was supported by colony-forming efficiency assay. Plating ZL55 SPT, SP and NSP cells resulted in the growth of two colony types: compact and loose (supplementary Figure 4 is available at *Carcinogenesis* Online). The yield of loose colonies was significantly ($P < 0.01$, Mann–Whitney test) higher in ZL55 SPT NSP compared with SP cells. SDM103T2 could not be analyzed in a similar way because cells grow spreading in the dish. However, a similar observation was obtained in ZL34 cells.

SP-derived tumors shift their expression toward mesothelium precursor phenotype

In order to get further insight into the mechanism of increased tumorigenic potential of SP-derived cells, gene expression and immunostaining was performed on SP- and NSP-derived tumors. The relative expression of mesothelioma markers calretinin (32), podoplanin (33) and mesothelin (31); ABC transporters ABCG2, MDR1 and ABCC1; stem cell markers Sox2, nestin, OCT4A, Bmi-1, CD90; sonic hedgehog activity markers Gli-1, Patch1; hypoxia controlled CAIX and Wisp2 and matrix-remodeling Slug, Twist and PAI-1 were investigated in 10 ZL55 SP- and NSP-derived tumors. Some mouse genes (Gli-1, Patch1 and Sca-1) were also included to take into account the mouse stromal components. Although of all the genes analyzed, only Patch1 was significantly enriched in SP-derived tumors ($P < 0.05$, two way analysis of variance), it nevertheless indicates that SP- and NSP-derived tumors are different and suggests the involvement of sonic hedgehog signaling. An unsupervised clustering showed separation of SP and NSP tumors (Figure 2B) with the exception of three tumors. In addition to Patch1, the expression of podoplanin was enriched in SP compared with NSP derived tumors. Latter observation was confirmed by immunostaining of tumor sections (Figure 2C and D and Table II) where we observed that podoplanin staining shifted from the membrane to the cytoplasm in SP derived tumors.

Mesothelioma is classified according to histopathology into epithelioid, biphasic and sarcomatoid subtype, with the biphasic type being defined as a tumor comprising >10% of both epithelioid and sarcomatoid areas (34). In SP-derived tumors, we observed a morphological shift from 100% epithelioid tumor to a mixed morphology for ZL55-derived tumors or to an increased spindeloid phenotype for SDM103T2 cells (Table II). The latter was paralleled by a significant decrease ($P < 0.01$) in cells with positive nuclear WT1 immunostaining (30 and 98% in ZL55- and SDM103T2-derived tumors, respectively). In contrast to observations *in vitro* where differences in mesothelin and N-cadherin expression were observed in SP and NSP fractions, all tumoral cells showed positive immunostaining for these markers (supplementary Figure 5 is available at *Carcinogenesis* Online). There can be many reasons for it, including growth in an *in vivo* environment. In addition, all tumors were positive for calretinin.

The resistance of stem-like cells to conventional chemotherapy is thought to be the cause of tumor recurrence. Hence, we investigated whether the recurrence tumor SDM141 from the patient SDM103, from which SDM103T2 were derived, would have a similar shift toward mesothelium precursor phenotype, defined here as the absence of WT1 expression, podoplanin shift from membrane to the cytosol and spindeloid phenotype. We observed indeed a loss of WT1 expression, an increased cytosolic podoplanin immunostaining and a shift toward sarcomatoid morphology in SDM141 sample compared with epithelioid SDM103 phenotype (Figure 2E). These observations indicate first that in the xenograft (SDM103T2) grown in mice, cells selected to grow were already shifting to spindeloid phenotype compared with parental tumor and second that xenografted SP cells behave like relapsing tumors, buttressing the hypothesis that relapse might be due to resistant cancer stem-like cells. Similar results were observed for tumor evolution in other two patients (supplementary Figure 6 is available at *Carcinogenesis* Online).

ZL55 SPT cells were more chemoresistant to chemotherapeutics

Since mesothelioma patients develop resistance against chemotherapy and because ABCG2 expression is correlated with a higher resistance to chemotherapeutics, we investigated the chemoresistance of ZL55 SPT and ZL55 NSPT3-3 cells. The latter were incubated either with verapamil, with mitoxantrone, a known ABCG2 substrate, or with a combination of verapamil and mitoxantrone (Figure 3A). ZL55 SPT cells were more resistant to mitoxantrone compared with ZL55 NSPT3-3 cells, but this difference was abolished ($P < 0.01$, paired *t*-test) in the presence of verapamil. Additionally, ZL55 SPT, and ZL55 NSPT3-3 cells were incubated with different concentrations of cisplatin, a chemotherapeutic agent commonly used for the treatment of mesothelioma patients. Also in this case, ZL55 SPT cells were significantly ($P < 0.001$, *t*-test) more resistant to a high concentration of cisplatin compared with ZL55 NSPT3-3 cells (Figure 3B). Cisplatin induced DNA damage was similar in both ZL55 SPT and NSPT3-3 cells as indicated by the phosphorylation of the histone variant H2AX (Figure 3C), occurring downstream DNA damage response (reviewed in ref. 35). However, a better survival in ZL55 SPT compared with NSPT3-3 cells was correlated with higher basal expression of survivin (Figure 3C), an antiapototic protein upregulated in MPM (36). In addition, cisplatin exposure resulted in a further increase of survivin levels, which contributes to chemoresistance, as we have described previously (37). All in all, these data indicate that SP derived cells are more chemoresistant.

SP cells are CD105$^{-/low}$

To gather more information on the SP phenotype, we determined whether mesenchymal stem cell (MSC) markers CD105, CD90 and CD73, which were expressed in all MPM investigated (Supplementary Table II is available at Carcinogenesis Online), would be differentially expressed in the SP itself. We also investigated the expression of podoplanin and of ABCG2, which were differentially expressed in the various cultures. The SP was specifically enriched in CD105$^{-/low}$ cells for SDM103T2 (4.9 ± 2.8-fold enrichment, $P < 0.05$, Mann–Whitney test, $n = 4$) (Figure 4A). Similar results were obtained for ZL55 cells. In addition, CD105$^{-/low}$ cells were smaller (Figure 4B). No specific enrichment was observed with the other two markers. Sorted ZL55 CD105$^{-/low}$ cells induced tumors which were five times larger ($P < 0.02$, $n = 4$, *t*-test) compared with CD105^{high} cells buttressing the existence of a cell subpopulation with high tumorigenic potential (Figure 4C). Consistent with this observation, Ki67 proliferation marker immunostaining was more abundant in ZL55 CD105$^{-/low}$ cells-derived tumors (Figure 4D).

Table II. Spindeloid cells and higher cytoplasmic podoplanin expression in ZL55 SP and SDM103T2 SP-derived tumors compared with contra laterally derived NSP tumors or parental cells

	Morphology		Podoplanin		
	Epithelioid	Spindeloid	Positive cells (%)	Mb	Cyt
Mouse 1					
ZL55 SPT3-3	90%	5–10%	5	+	++
ZL55 NSPT3-3	100%	0%	2–5	++	+
Mouse 2					
ZL55 SPT SPT2	95%	5%	30	++	++
ZL55 SPT NSPT	100%	0%	10	++	+
Mouse 3					
ZL55 SPT SPT3	95%	5%	80	+	++
ZL55 SPT NSPT2	100%	0%	30–40	++	+
SDM103T2	20	80	50	++	+
SDM103T2 SPT	10	90	10	+	+++
SDM103T2 SPT2	0	100	50	+	+++

Mb, membrane; Cyt, cytoplasmic.

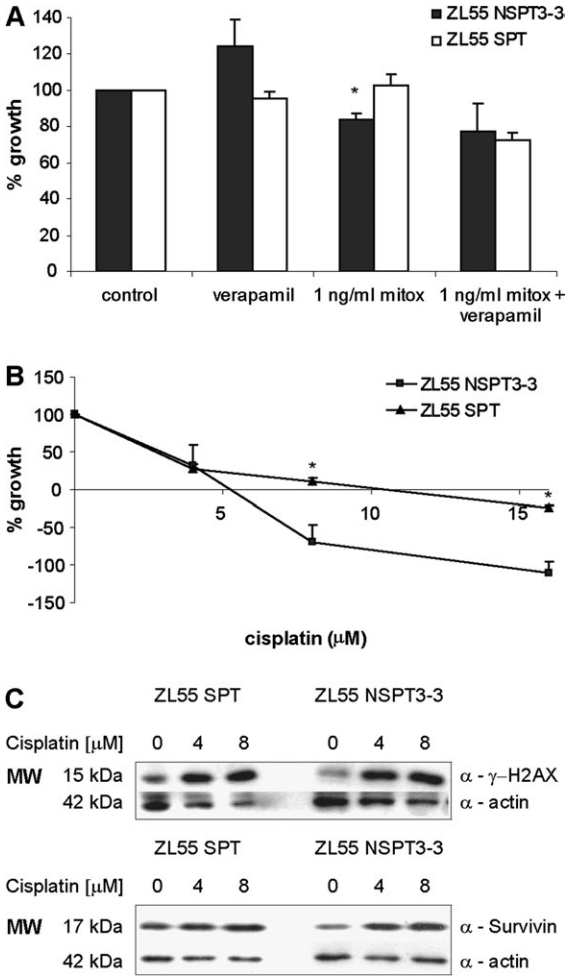

Fig. 3. SP-derived tumor cells are more chemoresistant (**A** and **B**) ZL55 SPT and NSPT3-3 cells were plated in 96-well plates and treated 24 h later with verapamil (50 μM), mitoxantrone (1 ng/ml) and a combination of the two for 1 h or with different cisplatin concentrations for 72 h. The MTT assay was performed 72 h after beginning of the drug treatment. ZL55 SPT-derived cells were more ($^*P < 0.01$) chemoresistant to mitoxantrone compared with NSPT3-3-derived cells and this difference was abolished by verapamil. ZL55 SPT cells were also more ($^*P < 0.001$) resistant against high doses of cisplatin. The data were normalized to the drug-untreated control. (**C**) Western blot analysis to assess the expression of the DNA damage sensing protein γH2AX biomarker (JBW301, 1:1000; Millipore, Zug, Switzerland, upper panel) and the survival protein survivin (Pab, 1:1000; R&D Systems, Abingdon, UK, lower panel). No difference in the γH2AX biomarker expression between the two lines was detected. ZL55 SPT cells showed higher basal survivin expression.

Discussion

In this study, we identified an SP with self-renewal and chemoresistance capacity, enriched in $CD105^{-/low}$ cells and able to induce, when implanted under the renal capsule of NOD/SCID mice, the growth of a tumor with increased spindeloid morphology. Furthermore, we observed that $CD105^{-/low}$ cells develop larger tumors compared with $CD105^{high}$ cells. Unfortunately, the yield of SP in $CD105^{-/low}$ cells was insufficient to allow any investigation of the double selection. However, based on current knowledge on embryonic mesothelium development, the proposed recruitment of adult precursor cells by asbestos (38) and on our own results, we put forward the hypothesis that MPM SP $CD105^{-/low}$ cells include mesothelioma cells responsible for tumor recurrence in patients (supplementary Figure 7 is available at *Carcinogenesis* Online).

MPM SP fractions varied between cell cultures but were in the same range of magnitude as found in other cancer types (39). They were enriched for ABCG2 transporter expression as observed by others (28,40) and the fraction of ABCG2 surface-positive cells was in a similar range as the SP fraction. In addition, the ABCG2-specific inhibitor fumitremorgin C (41) inhibited dye efflux (data not shown), therefore, it is likely that ABCG2 is responsible for the SP phenotype in MPM.

The epithelioid differentiation marker mesothelin was low in the SP fraction. Not much is known about the regulation of mesothelin expression. However, in MexTag mice in which the SV40 T-antigen (Tag) is under the control of the mesothelin promoter and which develop MPM tumors upon exposure to asbestos fibers, Tag is not detected in the unexposed mice (42). This may indicate that the cells that are stimulated to proliferate upon asbestos fibers exposure are undifferentiated precursor cells. The latter have been recently described in normal mesothelial primary cultures (43).

Similar to another study using MS-1 MPM cell line (15), no difference in tumorigenicity of SP versus NSP was observed, when starting material was a cell line. Nevertheless, tumors from xenograft-derived SP had a tendency to be more frequent but most importantly shifted toward a precursor phenotype defined here as enriched for podoplanin expression and low WT1 expression. It is noteworthy that podoplanin, also called D2-40 antigen, is a marker of splanchnic mesoderm (44) from where mesothelium derives. Hence, SP-derived tumors have an increased expression of mesothelium precursor marker. WT1 is a transcription factor expressed at the time of switch from mesenchymal to epithelial cells in mesothelium precursor cells (45). Continuous WT1 expression is conserved in mesothelium through adult life and is maintained in mesothelioma (46). However, it decreases during epithelial to mesenchymal transition occurring for example in sarcomatoid mesothelioma (47). Altogether, these data indicate that SP-derived tumors shift their expression toward mesothelium precursor phenotype.

Consistent with a mesenchymal–epithelial transition concept and precursors being of mesenchymal phenotype, SP-derived tumors shifted backwards from epithelioid to spindeloid morphology characterized by cytoplasmic podoplanin expression as observed by others (33,48–50) and decrease of nuclear WT1 staining (47).

This phenotype shift cannot be attributed to the microenvironment since such changes were not observed in NSP cells-derived tumors developed contra laterally. In addition, the increase in mesenchymal profile was consistent with the hypothesis that mesothelium injury, due to asbestos fibers accumulation in the pleural space, activates tissue repair involving MSC (38). It is possible, as suggested by Beachy *et al.*(4), that persistent injury and stimulation of repair would lead in such cells to oncogenic events, represented in our model by the loss of NF2 and INK4A function (reviewed in ref. 51).

Furthermore, we investigated MSC markers CD105, CD90 and CD73 expression in MPM cell lines and primary cell cultures. All investigated MPM cell lines and primary cell cultures were positive for all three MSC markers but only CD105 was differently expressed in SP and NSP: SP was enriched in $CD105^{-/low}$ cells. The latter developed larger tumors compared with $CD105^{high}$ cells. CD105 is an ancillary-transforming growth factor β receptor, and it is not clear whether its differential expression in MPM cells is responsible for the observed phenotype. In HSCs, CD105-positive cells contain all the long-term repopulating HSC activity within bone marrow SP (52), whereas others have suggested a function of CD105 as a tumor suppressor in epithelial cancer (53). Hence, functional studies are necessary to address any role of CD105 in MPM tumorigenicity. Intriguingly, $CD105^{-/low}$ cells had also a smaller size. This is in line with observation from Grichnik *et al.* who identified SP cells in metastatic melanoma cell lines which, compared with NSP cells, were small in size and gave rise to a heterogeneous cell population (54). A small size for stem-like cells has also been reported in glioma cells (30) and in squamous cell carcinoma (A431) cells (55).

Alternatively to the hypothesis that asbestos fibers recruit and alter a mesothelium precursor, acquisition of oncogenic lesions may occur in terminally differentiated cells resulting in dedifferentiation to a primitive stem-like state. This state is often associated with

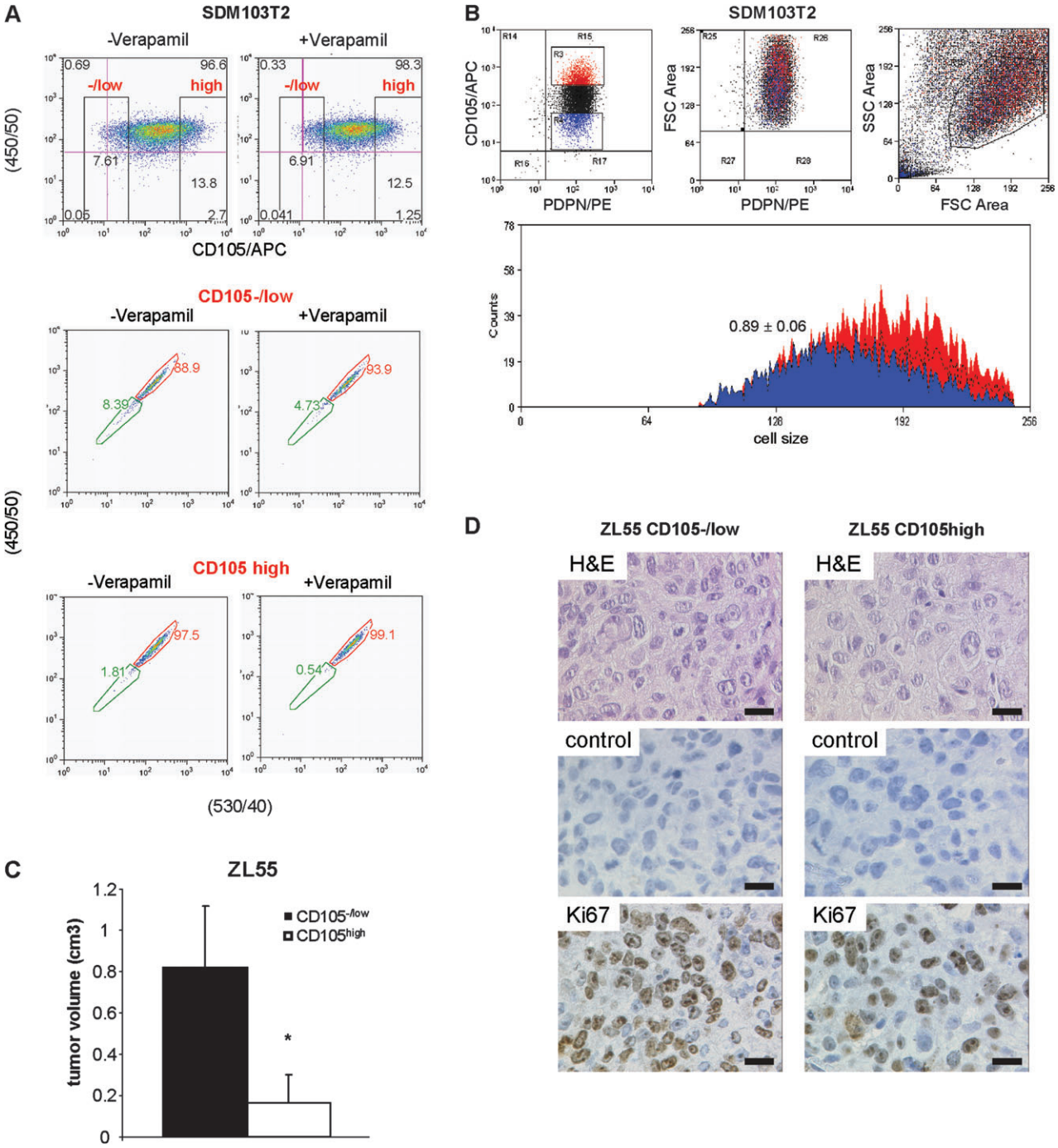

Fig. 4. SP cells are enriched in CD105$^{-/low}$ cells with increased tumorigenicity (**A**) The DCV efflux assay was performed to identify SP cells as indicated in the legend to Figure 1, followed by cell staining with an antibody against CD105 labeled with allophycocyanin (SN6) to identify CD105$^{-/low}$- and CD105^{high}-expressing cells. The SP fraction was then evaluated gating these two populations. (**B**) SDM103T2 cells were stained with anti-podoplanin and anti-CD105, then CD105$^{-/low}$ and CD105^{high} cells were analyzed in an Forward Scatter Channel Area histogram (cell size, lower panel) revealing that CD105$^{-/low}$ cells (blue) are smaller in cell size compared with CD105^{high} cells (red). Number above the cell size plot represents the cell size ratio of CD105$^{-/low}$ to CD105^{high} cells size ($n = 9$). (**C**) CD105$^{-/low}$- and CD105^{high}-expressing ZL55 cells were sorted, mixed with Matrigel and injected under the renal capsula of 1 Gy-irradiated NOD/SCID mice. Tumor volume was assessed after 12 weeks. CD105$^{-/low}$ cells induced significantly ($^{*}P < 0.02$) bigger tumors. (**D**) Increased proliferation in representative CD105$^{-/low}$- and CD105^{high}-derived tumors was buttressed by staining with a proliferation marker Ki67 antibody (B126.1, 1:50; Abcam). No primary antibody was added in controls. The scale bar represents 20 μm.

epithelial to mesenchymal transition and chemoresistance (56) like observed in our study. It would be interesting to further investigate the potential of induction of differentiation as therapeutic option. In this context, it is noteworthy that all-*trans*-retinoic acid treatment decreased growth of a sarcomatoid MPM cell line *in vivo* without induction of apoptosis (57). Since WT1 is controlled by retinoic acid (58), one possibility which remains unexplored is that WT1 was induced and it led to tumor cell differentiation and growth arrest.

Taken together, our results support the hypothesis that MPM recurrence develops from mesothelium precursor-like cells. But most importantly, we rise for the first time an issue that is seldom taken into account in mesothelioma biology: mesothelium has mesodermal

origin and undergoes mesenchymal to epithelial transition during development. Mesothelioma progression from epithelioid to biphasic to sarcomatoid seems to follow a 'backward to precursor' epithelial to mesenchymal transition, which for the moment has not been thoroughly addressed because of the complexity of mesothelium itself which maintains some mesenchymal characteristics (e.g. vimentin _expression). Using tools that are already largely used in the clinic such as immunohistochemistry for WT1 and podoplanin, we provide knowledge that could be easily implemented in large cohorts of patients to verify whether it could predict time to relapse and allow adaptation of patient follow-up.

Supplementary material

Supplementary Tables I and II and Figures 1–7 can be found at http://carcin.oxfordjournals.org/

Funding

Oncosuisse, the Zurich Krebsliga, Honegger and Sophien Foundations to R.S. and E.F.B. and ESMO fellowship to I.O.

Acknowledgements

We thank Dr Kisielow for skillfull assistance in FACS analysis, Dr Lukas Sommer for critical reading of the manuscript, Nicole Grosse-Frenzel for help for mice irradiation, Drs Andreev and Kerjaschki for providing HL60/Ddox cells and anti-podoplanin antibody, respectively.

Conflict of Interest Statement: None declared.

References

1. Peto,J. *et al*. (1999) The European mesothelioma epidemic. *Br. J. Cancer*, **79**, 666–672.
2. Stahel,R.A. *et al*. (2009) Improving the outcome in malignant pleural mesothelioma: nonaggressive or aggressive approach? *Curr. Opin. Oncol.*, **21**, 124–130.
3. van Meerbeeck,J.P. *et al*. (2011) Malignant pleural mesothelioma: the standard of care and challenges for future management. *Crit. Rev. Oncol. Hematol*. **78**, 92–111.
4. Beachy,P.A. *et al*. (2004) Tissue repair and stem cell renewal in carcinogenesis. *Nature*, **432**, 324–331.
5. Mossman,B. *et al*. (1983) Asbestos: mechanisms of toxicity and carcinogenicity in the respiratory tract. *Annu. Rev. Pharmacol. Toxicol.*, **23**, 595–615.
6. Donaldson,K. *et al*. (2010) Asbestos, carbon nanotubes and the pleural mesothelium: a review of the hypothesis regarding the role of long fibre retention in the parietal pleura, inflammation and mesothelioma. *Part. Fibre Toxicol.*, **7**, 5.
7. Reya,T. *et al*. (2001) Stem cells, cancer, and cancer stem cells. *Nature*, **414**, 105–111.
8. Lapidot,T. *et al*. (1994) A cell initiating human acute myeloid leukaemia after transplantation into SCID mice. *Nature*, **367**, 645–648.
9. Bonnet,D. *et al*. (1997) Human acute myeloid leukemia is organized as a hierarchy that originates from a primitive hematopoietic cell. *Nat. Med.*, **3**, 730–737.
10. Al-Hajj,M. *et al*. (2003) Prospective identification of tumorigenic breast cancer cells. *Proc. Natl Acad. Sci. USA*, **100**, 3983–3988.
11. Cho,R.W. *et al*. (2008) Recent advances in cancer stem cells. *Curr. Opin. Genet. Dev.*, **18**, 48–53.
12. Goodell,M.A. *et al*. (1996) Isolation and functional properties of murine hematopoietic stem cells that are replicating *in vivo*. *J. Exp. Med.*, **183**, 1797–1806.
13. Zhou,S. *et al*. (2001) The ABC transporter Bcrp1/ABCG2 is expressed in a wide variety of stem cells and is a molecular determinant of the side-population phenotype. *Nat. Med.*, **7**, 1028–1034.
14. Scharenberg,C.W. *et al*. (2002) The ABCG2 transporter is an efficient Hoechst 33342 efflux pump and is preferentially expressed by immature human hematopoietic progenitors. *Blood*, **99**, 507–512.
15. Kai,K. *et al*. (2010) Characterization of side population cells in human malignant mesothelioma cell lines. *Lung Cancer*, **70**, 146–151.
16. Thurneysen,C. *et al*. (2009) Functional inactivation of NF2/merlin in human mesothelioma. *Lung Cancer*, **64**, 140–147.
17. Sidi,R. *et al*. (2011) Induction of senescence markers after neo-adjuvant chemotherapy of malignant pleural mesothelioma and association with clinical outcome: an exploratory analysis. *Eur. J. Cancer*, **47**, 326–332.
18. Connell,N.D. *et al*. (1983) Regulation of the cytoskeleton in mesothelial cells: reversible loss of keratin and increase in vimentin during rapid growth in culture. *Cell*, **34**, 245–253.
19. Schmitter,D. *et al*. (1992) Hematopoietic growth factors secreted by seven human pleural mesothelioma cell lines: interleukin-6 production as a common feature. *Int. J. Cancer*, **51**, 296–301.
20. Ke,Y. *et al*. (1989) Establishment of a human *in vitro* mesothelial cell model system for investigating mechanisms of asbestos-induced mesothelioma. *Am. J. Pathol.*, **134**, 979–991.
21. Belyanskaya,L.L. *et al*. (2007) Human agonistic TRAIL receptor antibodies Mapatumumab and Lexatumumab induce apoptosis in malignant mesothelioma and act synergistically with cisplatin. *Mol. Cancer*, **6**, 66.
22. Goodell,M.A. (2002) Multipotential stem cells and ′side population′ cells. *Cytotherapy*, **4**, 507–508.
23. Telford,W.G. *et al*. (2007) Side population analysis using a violet-excited cell-permeable DNA binding dye. *Stem Cells*, **25**, 1029–1036.
24. Morgan,J. *et al*. (2010) Substrate affinity of photosensitizers derived from Chlorophyll-a: the ABCG2 transporter affects the phototoxic response of side population stem cell-like cancer cells to Photodynamic Therapy. *Mol. Pharm,* in press.
25. Watson,J.V. *et al*. (1985) Flow cytometric fluorescence emission spectrum analysis of Hoechst-33342-stained DNA in chicken thymocytes. *Cytometry*, **6**, 310–315.
26. Ozvegy-Laczka,C. *et al*. (2005) Function-dependent conformational changes of the ABCG2 multidrug transporter modify its interaction with a monoclonal antibody on the cell surface. *J. Biol. Chem.*, **280**, 4219–4227.
27. O'Brien,C.A. *et al*. (2007) A human colon cancer cell capable of initiating tumour growth in immunodeficient mice. *Nature*, **445**, 106–110.
28. Patrawala,L. *et al*. (2005) Side population is enriched in tumorigenic, stem-like cancer cells, whereas ABCG2+ and ABCG2- cancer cells are similarly tumorigenic. *Cancer Res.*, **65**, 6207–6219.
29. Montanaro,F. *et al*. (2004) Demystifying SP cell purification: viability, yield, and phenotype are defined by isolation parameters. *Exp. Cell Res.*, **298**, 144–154.
30. Kondo,T. *et al*. (2004) Persistence of a small subpopulation of cancer stem-like cells in the C6 glioma cell line. *Proc. Natl Acad. Sci. USA*, **101**, 781–786.
31. Chang,K. *et al*. (1996) Molecular cloning of mesothelin, a differentiation antigen present on mesothelium, mesotheliomas, and ovarian cancers. *Proc. Natl Acad. Sci. USA*, **93**, 136–140.
32. Doglioni,C. *et al*. (1996) Calretinin: a novel immunocytochemical marker for mesothelioma. *Am. J. Surg. Pathol.*, **20**, 1037–1046.
33. Chu,A.Y. *et al*. (2005) Utility of D2-40, a novel mesothelial marker, in the diagnosis of malignant mesothelioma. *Mod. Pathol.*, **18**, 105–110.
34. Travis,W. *et al*. (1999) WHO international histological classification of tumours: histological typing of lung and pleural tumours. 3rd edn. Springer-Verlag, Berlin, Germany
35. Jackson,S.P. *et al*. (2009) The DNA-damage response in human biology and disease. *Nature*, **461**, 1071–1078.
36. Falleni,M. *et al*. (2005) Quantitative evaluation of the apoptosis regulating genes Survivin, Bcl-2 and Bax in inflammatory and malignant pleural lesions. *Lung Cancer*, **48**, 211–216.
37. Belyanskaya,L.L. *et al*. (2005) Cisplatin activates Akt in small cell lung cancer cells and attenuates apoptosis by survivin upregulation. *Int. J. Cancer*, **117**, 755–763.
38. Mutsaers,S.E. (2002) Mesothelial cells: their structure, function and role in serosal repair. *Respirology*, **7**, 171–191.
39. Wu,C. *et al*. (2008) Side population cells in human cancers. *Cancer Lett.*, **268**, 1–9.
40. Hirschmann-Jax,C. *et al*. (2004) A distinct "side population" of cells with high drug efflux capacity in human tumor cells. *Proc. Natl Acad. Sci. USA*, **101**, 14228–14233.
41. Rabindran,S.K. *et al*. (2000) Fumitremorgin C reverses multidrug resistance in cells transfected with the breast cancer resistance protein. *Cancer Res.*, **60**, 47–50.
42. Robinson,C. *et al*. (2011) MexTAg mice exposed to asbestos develop cancer that faithfully replicates key features of the pathogenesis of human mesothelioma. *Eur. J. Cancer*, **47**, 151–161.

43. Lansley,S.M. *et al*. (2010) Mesothelial cell differention into osteoblast- and adipocyte-like cells. *J. Cell. Mol. Med.* doi: 10.1111/j.1582-4934.2010.01212.x.
44. Mahtab,E.A. *et al*. (2008) Cardiac malformations and myocardial abnormalities in podoplanin knockout mouse embryos: correlation with abnormal epicardial development. *Dev. Dyn.*, **237**, 847–857.
45. Hastie,N.D. (1994) The genetics of Wilms' tumor–a case of disrupted development. *Annu. Rev. Genet.*, **28**, 523–558.
46. Amin,K.M. *et al*. (1995) Wilms' tumor 1 susceptibility (WT1) gene products are selectively expressed in malignant mesothelioma. *Am. J. Pathol.*, **146**, 344–356.
47. Kumar-Singh,S. *et al*. (1997) WT1 mutation in malignant mesothelioma and WT1 immunoreactivity in relation to p53 and growth factor receptor expression, cell-type transition, and prognosis. *J. Pathol.*, **181**, 67–74.
48. Hinterberger,M. *et al*. (2007) D2-40 and calretinin - a tissue microarray analysis of 341 malignant mesotheliomas with emphasis on sarcomatoid differentiation. *Mod. Pathol.*, **20**, 248–255.
49. Padgett,D.M. *et al*. (2008) Podoplanin is a better immunohistochemical marker for sarcomatoid mesothelioma than calretinin. *Am. J. Surg. Pathol.*, **32**, 123–127.
50. Takeshima,Y. *et al*. (2009) Value of immunohistochemistry in the differential diagnosis of pleural sarcomatoid mesothelioma from lung sarcomatoid carcinoma. *Histopathology*, **54**, 667–676.
51. Stahel,R.A. *et al*. (2009) Malignant pleural mesothelioma. *Future Oncol.*, **5**, 391–402.
52. Chen,C.Z. *et al*. (2002) Identification of endoglin as a functional marker that defines long-term repopulating hematopoietic stem cells. *Proc. Natl Acad. Sci. USA*, **99**, 15468–15473.
53. Bernabeu,C. *et al*. (2009) The emerging role of TGF-beta superfamily coreceptors in cancer. *Biochim. Biophys. Acta*, **1792**, 954–973.
54. Grichnik,J.M. *et al*. (2006) Melanoma, a tumor based on a mutant stem cell? *J. Invest. Dermatol.*, **126**, 142–153.
55. Bortolomai,I. *et al*. (2010) Tumor initiating cells: development and critical characterization of a model derived from the A431 carcinoma cell line forming spheres in suspension. *Cell Cycle*, **9**, 1194–1206.
56. Singh,A. *et al*. (2010) EMT, cancer stem cells and drug resistance: an emerging axis of evil in the war on cancer. *Oncogene*, **29**, 4741–4751.
57. Tabata,C. *et al*. (2009) All-trans-retinoic acid inhibits tumour growth of malignant pleural mesothelioma in mice. *Eur. Respir. J.*, **34**, 1159–1167.
58. Bollig,F. *et al*. (2009) A highly conserved retinoic acid responsive element controls wt1a expression in the zebrafish pronephros. *Development*, **136**, 2883–2892.

Received April 14, 2011; revised May 31, 2011; accepted June 27, 2011